
Multi-Period Hierarchical Optimization for DER Dispatch in TSO-DSO Coordinated Networks

1st Martín Lucas Venegas
University of Santiago, Chile (USACH)
Santiago, Chile
martín.venegas@usach.cl

2nd Fernando García-Muñoz
University of Santiago, Chile (USACH)
Santiago, Chile
fernando.garciam@usach.cl

Abstract—This study proposes a hierarchical optimization model to coordinate Distributed Energy Resources (DERs) dispatch between Transmission System Operators (TSOs) and Distribution System Operators (DSOs), aiming to minimize operational costs, enable multi-period economic dispatch, optimize storage operations, and facilitate clean energy markets. In this regard, the TSO-DSO coordination is formulated as a bilevel optimization problem, where medium-voltage distribution networks (MV-DNs) act as leaders, optimizing DER operation based on load consumption and defining energy requirements for the TSO. The high-voltage transmission network (HV-TN) functions as a follower, dispatching DERs to meet the energy demands set by the MV-DNs. The DC optimal power flow (OPF) formulation is used to model HV-TN constraints, while the second-order cone relaxation of AC-OPF represents the MV-DN limitations. To address the nested complexity of the model, the Karush-Kuhn-Tucker (KKT) conditions and the Big-M method are applied to convert the bilevel problem into a single-level problem, making it computationally tractable. The model is tested on the IEEE 30-bus system for the HV-TN and the IEEE 33-bus system for the MV-DNs. The results demonstrate the model’s effectiveness in minimizing operational dispatch without voltage or congestion issues, with boundary variables satisfying equality constraints.

Index Terms—Hierarchical optimization, Energy market optimization, Distributed energy resources, Transmission network, Distribution network

I. INTRODUCTION

The ongoing decarbonization of the energy sector, driven by the need to reduce CO₂ emissions and mitigate climate change, demands a rapid and large-scale integration of zero-carbon energy sources [1], [2]. To meet global climate goals and limit global warming to 1.5°C, renewable generation must grow at an annual rate of 16.4% by 2030, with wind and solar expected to contribute at least 30% of electricity production [3], [4]. As Distributed Energy Resources (DERs), particularly renewable sources, are increasingly integrated into the power grid [1], they introduce new operational complexities. Their variability and decentralization challenge conventional planning and operation paradigms for both Transmission System Operators (TSOs) and Distribution System Operators (DSOs), leading to issues such as voltage deviations and congestion [5], [6].

These challenges are further exacerbated by sector electrification and the increasing interconnection between transmission and distribution levels, underscoring the need for improved TSO-DSO coordination [5]. DERs, however, also

offer significant flexibility, especially when integrated with storage and demand-side management systems. This flexibility has fostered the development of new mechanisms such as flexibility markets, where aggregators and energy communities support overall grid operation [7]. Yet, several research challenges remain: how to efficiently integrate DER flexibility into energy markets, how to coordinate decentralized DER operation, and how to design optimization models that ensure feasible and cost-effective coordination between TSOs and DSOs [5].

Thus, coordination schemes between TSOs and DSOs have been broadly classified as centralized, hybrid, and decentralized [8] to tackle these issues. Among them, decentralized and hierarchical structures have gained attention for reducing computational complexity while preserving operator autonomy [6]. These models often use linear or mixed-integer nonlinear programming, with Optimal Power Flow (OPF) constraints embedded to represent the physical characteristics of power networks. In this regard, recent literature emphasizes the potential of hierarchical optimization models, particularly those based on bilevel structures, where decision-making is distributed across multiple layers [9], [10]. These frameworks can incorporate both deterministic and stochastic elements depending on system uncertainty [11], [12], and are well-suited for scenarios with high DER penetration. Common solution techniques include the use of Karush-Kuhn-Tucker (KKT) conditions and the Big-M method to reformulate bilevel problems into single-level equivalents for tractable implementation [11], [13], [14].

This paper contributes to this growing body of work by proposing a hierarchical, multi-leader single-follower optimization model for coordinating the dispatch of DERs across interconnected TSO-DSO networks. In this setting, multiple DSOs act as independent leaders, optimizing their DER dispatch over multiple time periods, while the TSO, acting as the follower, adjusts the transmission-level dispatch to meet the aggregated energy requirements from the DSOs. This structure captures the decentralized decision-making logic of modern power systems while ensuring coordinated and feasible operation at the transmission level. The proposed model enables multi-period economic dispatch, incorporates storage operation, and serves as a foundation for more advanced market coordination schemes involving DERs.

The remainder of this paper is organized as follows: Section II describes the market framework and methodology. Section III details the mathematical formulation of the proposed optimization model. Section IV presents the case study and computational results. Finally, conclusions are drawn in Section V.

II. MARKET FRAMEWORK AND METHODOLOGY

This study assumes a hierarchical coordination framework between the TSO and the DSO for the dispatch of DER. The primary goal of the DSO is to optimize local DER operations, enabling multi-period economic dispatch and maximizing the utilization of distributed generation within distribution networks (DN). Meanwhile, the TSO focuses on integrating these optimization outcomes into the transmission network (TN) to maintain overall system stability. The coordination framework follows a bilevel approach, where the DSO acts as the leader, making operational decisions regarding DER management, including photovoltaic generation dispatch, energy storage, and demand response. In turn, the TSO adjusts TN dispatch according to the constraints imposed by the DN. This structure grants the DSO direct control over DERs within its area of influence while preserving the TSO's responsibility for system reliability and balance.

The model implements a day-ahead scheduling scheme, where the DSO transmits dispatch signals to the TSO. The TSO then performs adjustments to ensure transmission constraint compliance and maintain system operational security. Real-time information exchange between operators is essential to maintain consistency in decision-making across hierarchical levels. The proposed methodology for coordinating DER dispatch between the DSO and TSO is structured sequentially, advancing the development of a hierarchical optimization model focused on minimizing operational costs, enabling multi-period economic dispatch, optimizing storage operations, and supporting clean energy markets. The key stages of the methodology are as follows:

- 1) **Deterministic Economic Dispatch Model:** A bilevel optimization model is formulated to coordinate energy exchange between the TSO and a single DSO for a single time period. The DSO (leader) optimizes DER operations, while the TSO (follower) adjusts dispatch to meet the DSO's energy demands. To simplify computation, KKT conditions and the Big-M method are applied, transforming the bilevel problem into a single-level formulation. This model serves as the foundation for further developments.
- 2) **Extension to Multiple DSOs:** The model is expanded to consider two DNs, introducing the coordination of multiple DSOs. This extension accounts for interactions between distribution areas, enhancing the model's realism by reflecting the complexity of real-world power systems.
- 3) **Multiperiod Approach:** The base model is adapted to handle multiple time periods, capturing variations in

energy demand and supply while considering the integration of time-dependent DER operations.

- 4) **Incorporation of DER Technologies:** DERs such as batteries and solar panels are integrated into the model, enhancing flexibility and storage capacity within distribution networks. This inclusion also addresses the variability of solar generation and battery charging, enabling more accurate modeling of resource behavior.

III. OPTIMIZATION MODELS

The mathematical model presented below is an extended version of the bilevel optimization problem, which is transformed into a single-level problem. In this model, the DSO acts as the leader, and the TSO as the follower. This structure is possible because the problem can be represented as convex at the TSO level, allowing it to be treated as a follower within the optimization formulation. In this context, the DSO defines the energy requirements and the operation of DERs based on load consumption, while the TSO dispatches energy to meet those requirements. To address the hierarchical complexity of the model, KKT conditions and the Big-M method are applied to convert the bilevel problem into a single-level problem, making it computationally tractable. Additionally, constraints are incorporated for batteries and photovoltaic panels integrated into the distribution networks. In this formulation, the superscript D denotes variables and parameters related to the DSO, while the superscript T corresponds to those associated with the TSO.

The sets used in the mathematical model can be seen in Table 1. Since the model is being worked on in multiple periods, the constraints will apply $\forall t \in \mathcal{T}$.

Table 1
Sets Used in the Mathematical Model.

Symbol	Definition
$i \in \Omega_T$	Set of transmission system buses.
$i \in \Omega_B$	Set of boundary buses connecting the transmission and distribution systems; $\Omega_B \subset \Omega_T$.
$i \in \Omega_{D_k}$	Set of buses of the distribution system k , such that $k \in \Omega_B$.
$i \in \Omega_{B_k}$	Set of boundary buses of the distribution system k , such that $k \in \Omega_B$.
$(i, j) \in \mathcal{L}_T$	Set of transmission system lines, such that $\mathcal{L}_T = \{(i, j); i, j \in \Omega_T\}$.
$(i, j) \in \mathcal{L}_D$	Set of distribution system lines, such that $\mathcal{L}_D = \{(i, j); i, j \in \Omega_{D_k}\}$.
$t \in \mathcal{T}$	Set of time.

Objective Function:

$$\begin{aligned} \min z = & \sum_{t \in \mathcal{T}} \sum_{k \in \Omega_B} \sum_{i \in \Omega_{D_k}} C a_i (pv_{i,t}^D)^2 + C b_i (pv_{i,t}^D) + C c_i \\ & + \sum_{t \in \mathcal{T}} \sum_{k \in \Omega_B} \sum_{i \in \Omega_{B_k}} \pi (pg_{i,t}^B) \end{aligned} \quad (1)$$

In this model, the objective function, represented in expression (1), aims to minimize the costs associated with

energy generation at the buses of each DN, as well as to minimize the amount of energy transferred from one system to another at each substation. The active power generated by the photovoltaic panels (pv^D) contributes to the local energy supply, while the active power generated from the boundary bus (pg^B) represents the energy exchanged between interconnected networks. The generation costs of the unit are modeled as a quadratic function, where Ca , Cb , and Cc represent the quadratic, linear, and constant cost coefficients, respectively.

DSO Constraints:

$$\begin{aligned} & \sum_{(i,j) \in \mathcal{L}} p_{i,j,t}^D - \sum_{(j,i) \in \mathcal{L}} (p_{j,i,t}^D - R_{j,i}^D \ell_{j,i,t}^D) \\ & = \begin{cases} pv_{i,t}^D - ch_{i,t}^{Dbt} + ds_{i,t}^{Dbt} - PL_{i,t}^D & \forall i \in \Omega_D \\ pg_{i,t}^B & \forall i \in \Omega_B \end{cases} \end{aligned} \quad (2a)$$

$$\sum_{(i,j) \in \mathcal{L}} q_{i,j,t}^D - \sum_{(j,i) \in \mathcal{L}} (q_{j,i,t}^D - X_{j,i}^D \ell_{j,i,t}^D) = qg_{i,t}^D - QL_{i,t}^D \quad (2b)$$

$$\begin{aligned} v_{j,t}^D &= v_{i,t}^D - 2(R_{i,j}^D p_{i,j,t}^D + X_{i,j}^D q_{i,j,t}^D) \\ &+ (R_{i,j}^{D2} + X_{i,j}^{D2}) \ell_{j,i,t}^D \quad \forall (i,j) \in \mathcal{L}_D \end{aligned} \quad (2c)$$

$$(p_{i,j,t}^D)^2 + (q_{i,j,t}^D)^2 \leq \ell_{j,i,t}^D v_{i,t}^D \quad \forall (i,j) \in \mathcal{L}_D \quad (2d)$$

$$QG_i^{Dmin} \leq qg_{i,t}^D \leq QG_i^{Dmax} \quad \forall i \in \Omega_D \quad (2e)$$

$$V_i^{Dmin} \leq v_{i,t}^D \leq V_i^{Dmax} \quad \forall i \in \Omega_D \quad (2f)$$

$$\ell_{i,j,t}^D \leq I_{i,j}^{Dmax} \quad \forall (i,j) \in \mathcal{L}_D \quad (2g)$$

Constraint (2a) represents the active power balance at the bus, which varies depending on whether it is at a DN bus or a connection bus. The active power in the line between buses (p^D) captures the power transferred through the network, while the resistance between buses (R^D) and the current in the line (ℓ^D) influence the power losses. The active power load at the bus (PL^D) reflects the energy demand, while the charge and discharge power in the battery (ch^{Dbt} , ds^{Dbt}) account for the storage dynamics.

Constraint (2b) represents the reactive power balance at the DN bus $\forall i \in \Omega_D$, considering the reactive power in the line between buses (q^D) and the reactance between them (X^D). The reactive power generated at the bus (qg^D) contributes to meeting the reactive demand, while the reactive power load (QL^D) accounts for the consumption at the bus.

Constraints (2c) and (2d) represent the power flow relaxation, while constraints (2e) and (2f) establish the limits for reactive power and voltage at the bus, respectively. The voltage of the bus (v^D) must remain within the minimum and maximum allowable limits (V^{Dmin} , V^{Dmax}). Similarly, the reactive power generated at the bus is bounded by the minimum and maximum values (QG^{Dmin} , QG^{Dmax}). Finally, constraint (2g) defines the current capacity of the line, ensuring

that the current between buses does not exceed the maximum limit (I^{Dmax}).

Photovoltaic Panel Constraint:

$$pv_{i,t}^D \leq PV_t^{Dmax} \gamma_i^{Dpv} \quad \forall i \in \Omega_D \quad (3)$$

Constraint (3) represents the photovoltaic generation at the node, where the maximum active power (PV^{Dmax}) is limited by the panel capacity (γ^{Dpv}).

Battery Constraints:

$$soc_{i,t+1}^{Dbt} = soc_{i,t}^{Dbt} + (\varphi^{Dch} ch_{i,t}^{Dbt} - \frac{1}{\varphi^{Dds}} ds_{i,t}^{Dbt}) \Delta t \quad (4a)$$

$$SOC_{min}^{Dbt} \gamma_i^{Dbt} \leq soc_{i,t}^{Dbt} \leq SOC_{max}^{Dbt} \gamma_i^{Dbt} \quad (4b)$$

$$ch_{i,t}^{Dbt} \leq PB^{Dbt} (w_{i,t}^{Dbt}) \quad (4c)$$

$$ds_{i,t}^{Dbt} \leq PB^{Dbt} (1 - w_{i,t}^{Dbt}) - PB^{Dbt} (1 - \nu_i^{Dbt}) \quad (4d)$$

$$w_{i,t}^{Dbt} \leq \nu_i^{Dbt} \quad (4e)$$

Constraints (4a) and (4b) represent the battery state of charge and its stored charge limits, respectively. Meanwhile, constraints (4c) and (4d) represent the limits for charge and discharge. On the other hand, constraint (4e) allows deciding whether the battery charges or discharges if it is installed at the node. The battery state of charge (soc^{Dbt}) reflects the stored energy level, while the charging and discharging efficiencies (φ^{Dch} , φ^{Dds}) determine the effectiveness of each process. The minimum and maximum battery charge states (SOC_{min}^{Dbt} , SOC_{max}^{Dbt}) define the operational limits. The battery capacity (γ^{Dbt}) indicates the maximum energy storage potential, and the maximum charging/discharging power (PB^{Dbt}) limits the power exchange rate. A binary variable (w^{Dbt}) indicates whether the battery is discharging (1) or not (0), while another binary variable (ν^{Dbt}) denotes the presence of an installed battery. Constraints (4) apply $\forall i \in \Omega_D$.

Feasibility Conditions:

$$\sum_{(i,j) \in \mathcal{L}} p_{i,j,t}^T - pg_{i,t}^T + PL_{i,t}^T = 0 \quad : \lambda_{1,i,t} \in \mathbb{R} \quad (5a)$$

$$\sum_{(i,j) \in \mathcal{L}} p_{i,j,t}^T + pl_{i,t}^D = 0 \quad : \lambda_{2,i,t} \in \mathbb{R} \quad (5b)$$

$$X_{i,j}^T p_{i,j,t}^T - \theta_{i,t}^T + \theta_{j,t}^T = 0 \quad : \lambda_{3,i,j,t} \in \mathbb{R} \quad (5c)$$

$$p_{i,j,t}^T - S_{i,j}^{Tmax} \leq 0 \quad : \mu_{1,i,j,t} \geq 0 \quad (5d)$$

$$pg_{i,t}^T - PG_i^{Tmax} \leq 0 \quad : \mu_{2,i,t} \geq 0 \quad (5e)$$

$$pl_{i,t}^B - PL_i^{Bmax} \leq 0 \quad : \mu_{3,i,t} \geq 0 \quad (5f)$$

$$V_i^{Tmin} - v_{i,t}^T \leq 0 \quad : \mu_{4,i,t} \geq 0 \quad (5g)$$

$$v_{i,t}^T - V_i^{Tmax} \leq 0 \quad : \mu_{5,i,t} \geq 0 \quad (5h)$$

Constraints (5) arise after deriving the Lagrangian equation with respect to the vectors of KKT multipliers (μ and λ). The bus angle (θ^T) represents the voltage phase angle at the transmission bus, while the maximum apparent power (S^{Tmax}) defines the upper limit of power transfer between

buses. Constraints (5a), (5e), (5g) and (5h) apply $\forall i \in \Omega_T$. Constraints (5b) and (5f) apply $\forall i \in \Omega_B$. Finally, constraints (5c) and (5d) apply $\forall (i, j) \in \mathcal{L}_T$.

Stationary Conditions:

$$2Ca_i(pg_{i,t}^T) + Cb_i - \lambda_{1,i,t} + \mu_{2,i,t} = 0 \quad : pg_{i,t}^T \quad (6a)$$

$$\lambda_{2,i,t} + \mu_{3,i,t} = 0 \quad : pl_{i,t}^D \quad (6b)$$

$$\lambda_{1,i,t} + \lambda_{2,i,t} + \mu_{1,i,j,t} + \lambda_{3,i,j,t} X_{i,j}^T = 0 \quad : p_{i,j,t}^T \quad (6c)$$

$$\mu_{5,i,t} - \mu_{4,i,t} = 0 \quad : v_{i,t}^T \quad (6d)$$

$$\sum_{(i,j) \in \mathcal{L}} \lambda_{3,j,i,t} - \lambda_{3,i,j,t} = 0 \quad : \theta_{i,j,t}^T \quad (6e)$$

Constraints (6) arise after deriving the Lagrangian equation with respect to the variables of the problem. Constraints (6a) and (6d) apply $\forall i \in \Omega_T$. Constraint (6b) applies $\forall i \in \Omega_B$. Finally, constraints (6c) and (6e) apply $\forall (i, j) \in \mathcal{L}_T$.

Boundary Constraints:

$$pl_{k,t}^D = pg_{i,t}^B \quad \forall k \in \Omega_B, \forall i \in \Omega_{B_k} \quad (7)$$

Constraint (7) represents the condition where the demand at the connection bus must be equal to the power supplied by the substation at that connection bus. The active power load of the distribution network (pl^D) ensures that the power balance is maintained between the substation and the connected network.

Big-M Slack Conditions:

$$p_{i,j,t}^T - S_{i,j}^{Tmax} \leq M(1 - \alpha_{1,i,j,t}) \quad : \alpha_{1,i,j,t} \in [0, 1] \quad (8a)$$

$$\mu_{1,i,j,t} \leq M(\alpha_{1,i,j,t}) \quad : \alpha_{1,i,j,t} \in [0, 1] \quad (8b)$$

$$pg_{i,t}^T - PG_i^{Tmax} \leq M(1 - \alpha_{2,i,t}) \quad : \alpha_{2,i,t} \in [0, 1] \quad (8c)$$

$$\mu_{2,i,t} \leq M(\alpha_{2,i,t}) \quad : \alpha_{2,i,t} \in [0, 1] \quad (8d)$$

$$pl_{i,t}^D - PL_i^{Bmax} \leq M(1 - \alpha_{3,i,t}) \quad : \alpha_{3,i,t} \in [0, 1] \quad (8e)$$

$$\mu_{3,i,t} \leq M(\alpha_{3,i,t}) \quad : \alpha_{3,i,t} \in [0, 1] \quad (8f)$$

$$V_i^{Tmin} - v_{i,t}^T \leq M(1 - \alpha_{4,i,t}) \quad : \alpha_{4,i,t} \in [0, 1] \quad (8g)$$

$$\mu_{4,i,t} \leq M(\alpha_{4,i,t}) \quad : \alpha_{4,i,t} \in [0, 1] \quad (8h)$$

$$v_{i,t}^T - V_i^{Tmax} \leq M(1 - \alpha_{5,i,t}) \quad : \alpha_{5,i,t} \in [0, 1] \quad (8i)$$

$$\mu_{5,i,t} \leq M(\alpha_{5,i,t}) \quad : \alpha_{5,i,t} \in [0, 1] \quad (8j)$$

Constraints (8) arise after applying the Big-M method to linearize the original balance conditions. The Big-M constant (M) is a large positive number used to enforce the activation or deactivation of specific constraints. Continuous variables (α) take values within the interval $[0,1]$, representing proportional factors that influence the linearization process. Constraints (8a) and (8b) apply $\forall (i, j) \in \mathcal{L}_T$. Constraints (8c), (8d), and (8g) to (8j) apply $\forall i \in \Omega_T$. Finally, constraints (8e) and (8f) apply $\forall i \in \Omega_B$.

IV. CASE STUDY AND COMPUTATIONAL RESULTS

The model was implemented in Python-Pyomo using the Gurobi 10.0.3 solver and executed on an AMD Ryzen 5 7600X (4.70 GHz, 32 GB RAM).

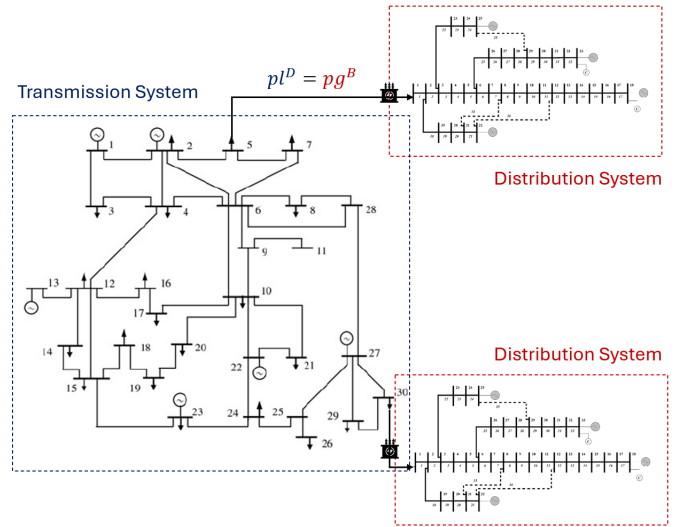


Fig. 1. Case Study. Schematic Representation TSO-DSO.

The model was tested on the IEEE 30-bus HV-TN and IEEE 33-bus MV-DNs (Fig. 1), with DNs connected at TN nodes 4 and 21. Each DN includes 20 batteries and 28 photovoltaic panels, with a 24-hour operation period.

The optimal objective value ranges from 51,876.4657 to 51,876.7795 [\$], with a reported lower bound of 51,876.47 [\$]. The problem, consisting of 42,528 constraints and 31,009 variables (binary, integer, continuous), was solved optimally in 0.665 seconds, demonstrating excellent convergence and scalability.

Power flows remain within capacity limits, indicating no congestion, while voltage levels in both TN and DNs stay within the 0.95–1.05 p.u. range, reflecting stable and efficient operation. Solar generation helps stabilize voltage during peak hours, while dips occur with high demand and low solar output.

Figure 2 illustrates the energy generation and demand curves for the DNs throughout the day. Energy generation follows a characteristic solar capture pattern, starting to increase around 6:00 AM, reaching its peak between 11:00 AM and 3:00 PM, and gradually decreasing until it ceases around 7:00 PM. However, the energy demand curves exhibit two significant peaks: the first between 6:00 and 10:00 AM and the second between 5:00 and 10:00 PM, with a maximum demand around 6:00 PM.

In the analysis of charging (CH) and discharging (DS) power, the batteries begin charging between 10:00 AM and 3:00 PM, with a peak close to 0.2 MW. This coincides with periods of high solar generation, suggesting that the batteries store the excess renewable energy available during these hours.

Regarding discharge, two main peaks are observed: the first around 7:00 AM, with both networks showing strong discharges near 0.35 MW, indicating that the batteries provide energy to the system to cover the initial demand peak. The second peak occurs around 6:00 PM, coinciding with the

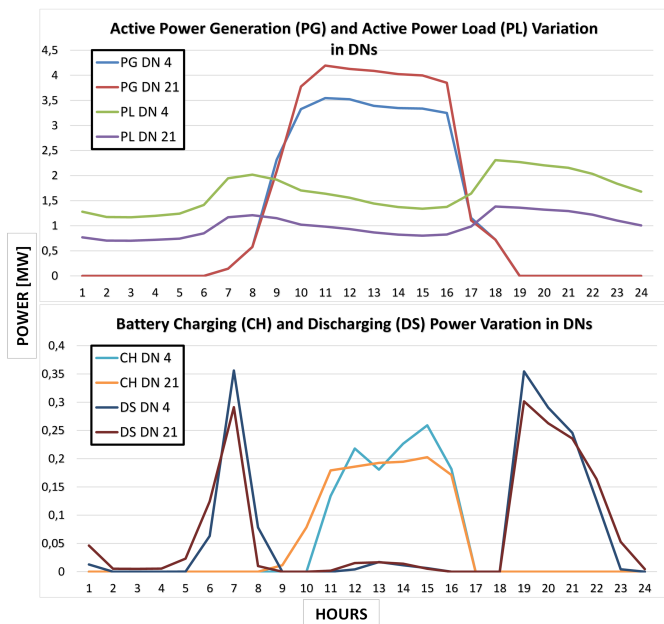


Fig. 2. Analysis of Power Variation in DN nodes: Active Generation, Demand, and Battery Management.

second period of high electrical demand. After these discharge peaks, the power gradually decreases.

This charging and discharging pattern reflects an efficient use of energy storage, aligned with solar generation and system demands. Batteries store energy when solar generation is abundant and release it during peak consumption hours, contributing to the stabilization of the electrical system.

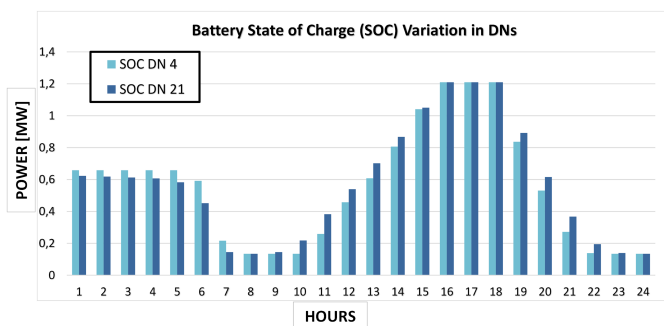


Fig. 3. Daily State of Charge Pattern of Batteries in DN nodes.

The state of charge (SOC) of the batteries in the DN nodes follows a daily pattern determined by the availability of solar generation. During the night (12:00 AM - 6:00 AM), the absence of solar radiation prevents battery recharging, leading to a progressive discharge to meet system demand. At sunrise (6:00 AM - 9:00 AM), the gradual increase in photovoltaic generation reduces the need for discharge, stabilizing the SOC. During peak radiation hours (10:00 AM - 3:00 PM), solar generation is sufficient to cover the demand and charge the batteries, resulting in an increase in SOC. Finally, in the afternoon (4:00 PM - 6:00 PM), the decline in radiation

reduces generation capacity, causing the batteries to discharge again to maintain energy supply, as illustrated in Figure 3.

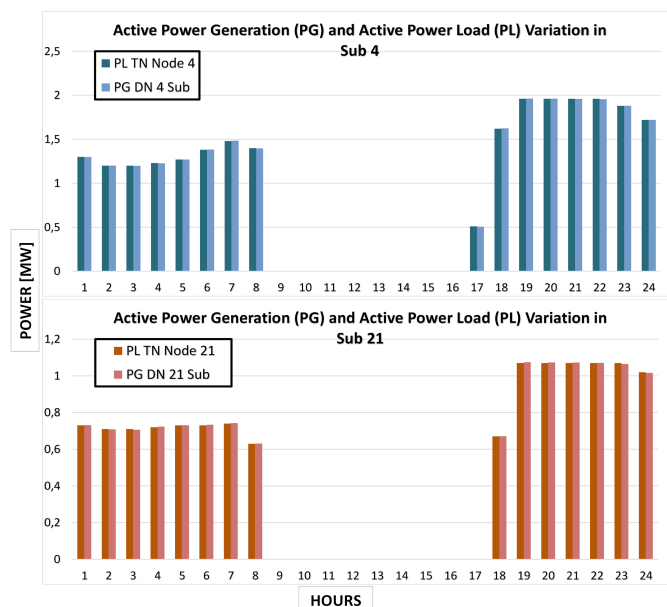


Fig. 4. Equality of Boundary Variables: Demand at DN Nodes 4 and 21 Matched with Generation at Substations.

Finally, as shown in Figure 4, the boundary variable equality condition is satisfied, ensuring that the demand of the DN nodes at nodes 4 and 21 matches the generation at their respective substations. This suggests proper TSO-DSO coordination, without imbalances.

V. CONCLUSIONS

The energy transition presents substantial operational challenges, primarily due to the intermittency of renewable energy sources and the limited preparedness of existing grid infrastructure. This work proposes a hierarchical, multi-period optimization model for coordinating DER operation between TSO and DSOs, maximizing efficiency and resource utilization. Preliminary results from IEEE test cases demonstrate the model's effectiveness in managing operational complexity, ensuring grid stability, and preventing voltage and congestion issues.

To enhance its applicability, future work should assess scalability on larger networks, incorporate market prices and regulatory constraints, and explore alternative optimization techniques to address numerical challenges. Expanding the model to include more diverse DERs and peer-to-peer trading could further increase flexibility and resilience. This study contributes to modern power networks by proposing an efficient and adaptable framework for TSO-DSO coordination and DER integration.

ACKNOWLEDGMENT

This work has been supported by ANID FONDECYT Iniciación 11240745. Additional support has been provided by the Vice-Rectorate for Postgraduate Studies of the University of Santiago, Chile.

REFERENCES

- [1] E. Papadis and G. Tsatsaronis, "Challenges in the decarbonization of the energy sector," *Energy*, vol. 205, p. 118025, 2020.
- [2] International Renewable Energy Agency (IRENA), "Energy transition outlook," 2024, retrieved on November 18, 2024, from <https://www.irena.org/Energy-Transition/Outlook>.
- [3] —, "Tripling renewables by 2030 requires a minimum of 16.4% annual growth rate," 2024, retrieved on November 18, 2024, from <https://www.irena.org/News/pressreleases/2024/Jul/Tripling-Renewables-by-2030-Requires-a-Minimum-of-16-point-4-pc-Annual-Growth-Rate-ES>.
- [4] International Energy Agency (IEA), "Renewables 2024," Paris, 2024, retrieved from <https://www.iea.org/reports/renewables-2024>, Licence: CC BY 4.0.
- [5] L. Lind, "Tso-dso coordination: a multidimensional study on coordination schemes, modelling and regulation in the european context," 2024.
- [6] G. K. Papazoglou, E. A. Bakirtzis, A. A. Forouli, P. N. Biskas, and A. G. Bakirtzis, "A two-stage market-based tso-dso coordination framework," in *2022 2nd International Conference on Energy Transition in the Mediterranean Area (SyNERGY MED)*. IEEE, 2022, pp. 1–6.
- [7] L. Lind, R. Cossent, J. P. Chaves-Ávila, and T. Gómez San Román, "Transmission and distribution coordination in power systems with high shares of distributed energy resources providing balancing and congestion management services," *Wiley Interdisciplinary Reviews: Energy and Environment*, vol. 8, no. 6, p. e357, 2019.
- [8] A. G. Givisiez, K. Petrou, and L. F. Ochoa, "A review on tso-dso coordination models and solution techniques," *Electric Power Systems Research*, vol. 189, p. 106659, 2020.
- [9] Z. Yuan and M. R. Hesamzadeh, "Hierarchical coordination of tso-dso economic dispatch considering large-scale integration of distributed energy resources," *Applied energy*, vol. 195, pp. 600–615, 2017.
- [10] O. K. Olsen, D. Sieraszewski, D. Ivanko, I. Oleinikova, and H. Farahmand, "Hybrid ac/dc optimal power flow modelling approach for coordination in flexibility market," in *2021 International Conference on Smart Energy Systems and Technologies (SEST)*. IEEE, 2021, pp. 1–6.
- [11] H. Chen, D. Wang, R. Zhang, T. Jiang, and X. Li, "Optimal participation of adn in energy and reserve markets considering tso-dso interface and ders uncertainties," *Applied Energy*, vol. 308, p. 118319, 2022.
- [12] K. Steriotis, P. Makris, G. Tsaousoglou, N. Efthymiopoulos, and E. Vavvarigos, "Co-optimization of distributed renewable energy and storage investment decisions in a tso-dso coordination framework," *IEEE Transactions on Power Systems*, vol. 38, no. 5, pp. 4515–4529, 2022.
- [13] S. Boyd, L. Xiao, A. Mutapic, and J. Mattingley, "Notes on decomposition methods," *Notes for EE364B, Stanford University*, vol. 635, pp. 1–36, 2007.
- [14] S. A. Mansouri, E. Nematbakhsh, A. R. Jordehi, M. Marzband, M. Tostado-Véliz, and F. Jurado, "An interval-based nested optimization framework for deriving flexibility from smart buildings and electric vehicle fleets in the tso-dso coordination," *Applied Energy*, vol. 341, p. 121062, 2023.